

A dynamical order parameter for the transition to nonergodic dynamics in the discrete nonlinear Schrödinger equation

Andrew Kalish, Pedro Fittipaldi de Castro, and Wladimir A. Benalcazar*

Department of Physics, Emory University, Atlanta, Georgia 30322, USA

(Dated: December 9, 2025)

The discrete nonlinear Schrödinger equation (DNLSE) exhibits a transition from ergodic, delocalized dynamics to a weakly nonergodic regime characterized by breather formation; yet, a precise characterization of this transition has remained elusive. By sampling many microcanonically equivalent initial conditions, we identify the asymptotic ensemble variance of the Kolmogorov–Sinai entropy as a dynamical order parameter that vanishes in the ergodic phase and becomes finite once ergodicity is broken. The relaxation time governing the ensemble convergence of the KS entropy displays an essential singularity at the transition, yielding a sharp boundary between the two dynamical regimes. This framework provides a trajectory-independent method for detecting ergodicity breaking that is broadly applicable to nonlinear lattice systems with conserved quantities.

The one-dimensional discrete nonlinear Schrödinger equation (DNLSE) exhibits two thermodynamically distinct regions separated by an infinite-temperature line [1]: a positive-temperature Gibbs phase, where canonical and microcanonical ensembles are equivalent, and a non-Gibbs region where the canonical partition function diverges and only the microcanonical ensemble is well defined.

Throughout the Gibbs phase, the long-time dynamics are delocalized and appear ergodic. Within the non-Gibbs region, approximate microcanonical entropy calculations show that energy localization becomes favored at high energies, concentrating a finite fraction of the total energy onto one or a few sites [1, 2]. At sufficiently large energy densities, these localized configurations (breathers) become dynamically stable, leading to weakly nonergodic behavior, in which microcanonically equivalent initial conditions fail to explore the same regions of phase space [3]. Despite these advances, a precise characterization of ergodicity breaking in the DNLSE as a dynamical phase transition remains lacking.

In this Letter, we approach the problem from an ensemble perspective. Instead of diagnosing ergodicity breaking from the statistics of individual trajectories, we sample many initial conditions at fixed energy and norm and monitor how their finite-time Kolmogorov–Sinai (KS) entropies evolve. This reveals how dynamical heterogeneity develops across the microcanonical manifold and allows us to sharply distinguish ergodic from nonergodic behavior. We show that ensemble variance of the KS entropy acquires a finite asymptotic value only when energy becomes trapped in sufficiently stable breather excitations, and that the corresponding relaxation time diverges with an essential singularity at the transition. This construction yields a trajectory-independent dynamical order parameter and provides a general tool for identifying ergodicity-breaking transitions in nonlinear Hamiltonian lattices.

The DNLSE, interchangeably referred to as the discrete Gross-Pitaevskii equation, or semiclassical Bose-

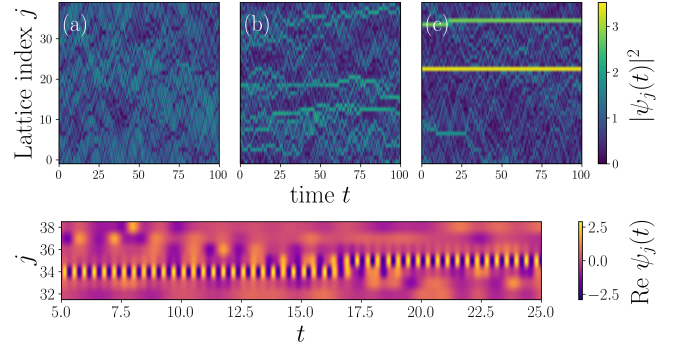


FIG. 1. **Time evolution of a state ψ under the discrete nonlinear Schrödinger equation**, Eq. (1), shown for (a) delocalized, (b) pseudo-localized, and (c) localized phases. The lattice size $N = 40$ and amplitude density $a = 1$ are fixed while energy densities are $e = 0.8, 2.3, 5.5$ from left to right. Bottom: Real component $\text{Re } \psi_j(t)$ of the smaller breather evolution in c.

Hubbard model, is a semiclassical mean-field model describing weakly interacting bosons in discrete geometries, such as Bose-Einstein condensates confined to optical lattices. Its equation of motion is

$$i\dot{\psi}_j = -h(\psi_{j+1} + \psi_{j-1}) - g|\psi_j|^2\psi_j, \quad j = 1, \dots, N \quad (1)$$

with $g, h > 0$, describing the time evolution of a complex-valued field $\psi = (\psi_1, \dots, \psi_N) \in \mathbb{C}^N$ on an N -site 1-dimensional lattice with periodic boundary conditions, where squared amplitudes $|\psi_j|^2$ represent the particle density on the j th lattice site. The DNLSE has broad relevance in physics beyond Bose condensates; notably, it is also utilized as a model of light propagation in waveguide arrays with Kerr nonlinearity [4, 5], and has found diverse applications elsewhere, including plasma physics [6], acoustics [7], and biophysics [8].

The system of equations (1) is invariant under global $U(1)$ phase rotation as well as time translation. The former symmetry corresponds with conservation of total particle number $\|\psi\|^2 = \sum_{j=1}^N |\psi_j|^2$, while the latter

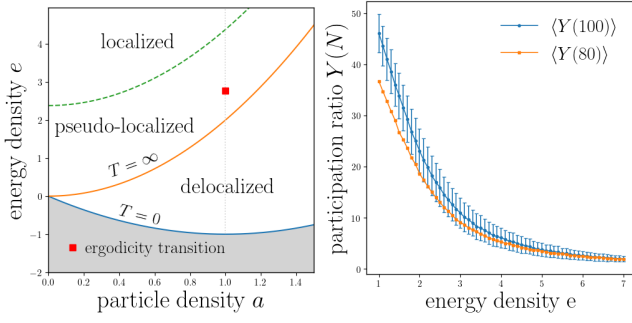


FIG. 2. **Phase diagram in (e, a) space.** Ground state and infinite temperature isotherm was identified in [2]. Breather localizations are still persistent in the pseudo-localized phase; however, the participation ratio (right, shown for $a = 1$) is extensive for all states below the green dashed curve identified by [1], which approaches the $T = \infty$ boundary as $N \rightarrow \infty$. Evolutions in each phase are shown in Fig. 1. Left: Ensemble averages and standard deviations of the participation ratio $Y(N)$

implies conservation of the Hamiltonian

$$H = \sum_{j=1}^N h(\psi_j^* \psi_{j+1} + \psi_{j+1}^* \psi_j) + \frac{g}{2} |\psi_j|^4. \quad (2)$$

Here $\{\psi_j, i\psi_j^*\}$ are the conjugate variables and $i\psi_j = -\partial H / \partial \psi_j^*$ recovers the equation of motion (1). The thermodynamic state is specified by the conserved densities $a = \|\psi\|^2 / N$ and $e = H / N$. Throughout this work, we set $h = 1$ and $g = 2$, and focus on the $a = 1$ slice of the phase diagram shown in Fig. 2.

Given the pair of conserved quantities in the DNLSE, we seek to determine for which values of (e, a) is the microcanonical set $\mathcal{M}_{e,a}^{(N)} := \{\psi \in \mathbb{C}^N : H(\psi) / N = e, \|\psi\|^2 / N = a\}$ ergodic. For ergodic states, a relaxation time can be quantified with respect to the rate at which the variance of some observable across all states in \mathcal{M} vanishes, and for nonergodic states there must exist some observable whose distribution maintains a finite variance asymptotically.

Prior quantitative studies of ergodicity breaking in the DNLSE have relied on single-trajectory statistics of excursion times off of Poincaré manifolds [3], which, while demonstrating nonergodic behavior, face significant limitations. Our complementary approach - involving global statistics across hundreds of microcanonically equivalent initial conditions - offers a clearer picture of the transition. In particular, our framework allows for characterizing the divergence in relaxation times as the transition is approached, and further provides a metric of the "strength" of broken ergodicity throughout the nonergodic phase.

Our approach to the study of ergodicity breaking in this system begins with sampling initial conditions from the microcanonical ensemble; that is, assigning a uniform

probability weight to all states in $\mathcal{M}_{e,a}^{(N)}$. For even small values of N an exact sampling of \mathcal{M} is not feasible, and a Markov chain Monte-Carlo method is appropriate, which we discuss first. For convenience, we define the function $F : \mathbb{C}^N \rightarrow \mathbb{R}^2$, $F(\psi) := (H(\psi), \|\psi\|^2) = (E, A)$, which maps a state to its conserved quantities. (We may sometimes abuse notation and also write A to mean the function $A(\psi) = \|\psi\|^2$, however, this should be clear from context.) Note that the microcanonical partition function may be written as

$$\int_{\mathbb{C}^N} \delta(F(\psi) - (E, A)) d\psi = \int_{F^{-1}(E, A)} \frac{d\sigma(\psi)}{\|\nabla H(\psi) \wedge \nabla A(\psi)\|}, \quad (3)$$

where $d\psi = \prod_j d(\text{Re}\psi_j) \cdot d(\text{Im}\psi_j)$, $d\sigma$ is formally the $2N - 2$ dimensional Hausdorff measure, and $F^{-1}(E, A) = \mathcal{M}_{e,a}^{(N)}$ is a differentiable manifold at almost every (E, A) by Sard's theorem [9–11]. To sample from the microcanonical ensemble, we implement a random walk on the manifold $\mathcal{M}_{e,a}^{(N)}$ with an acceptance probability of a step from $\psi \rightarrow \psi'$ being

$$p(\psi \rightarrow \psi') = \min \left(1, \frac{\|\nabla H(\psi') \wedge \nabla A(\psi')\|}{\|\nabla H(\psi) \wedge \nabla A(\psi)\|} \cdot \frac{\alpha(\psi' \rightarrow \psi)}{\alpha(\psi \rightarrow \psi')} \right), \quad (4)$$

where the factors α correct for any asymmetry in the proposals. Put concisely, we implement a Metropolis-Hastings chain [12, 13] targeting the stationary distribution $p(\psi) \propto 1 / \|\nabla H(\psi) \wedge \nabla A(\psi)\|$. Our method of implementing this sampling procedure, in particular our approximation of α , and further details about this representation of the partition function are included in the supplementary material. Sampling in this manner gives a finite set of microcanonically weighted states which serve as a representative subset of \mathcal{M} .

For a range of energies, we sample between many initial conditions from $\mathcal{M}_{e,a}^{(N)}$, and for each sampled state we compute the finite-time Lyapunov spectrum $\{\lambda_j(t)\}_{j=1}^{2N}$ and the Kolmogorov-Sinai entropy $S_{KS} \equiv \sum_{\lambda_j > 0} \lambda_j(t)$.

Lyapunov exponents are real-valued with units of inverse time, and describe local stretching rates about a trajectory - with each λ_j corresponding to an orthogonal degree of freedom in the tangent space of $\psi(t)$. They can be thought of as factors describing the strength of chaos, where commonly a single positive Lyapunov exponent is considered a sufficient condition for dynamics to be deemed chaotic.

Zero-valued Lyapunov exponents correspond to conserved quantities, and near-zero exponents appear in the presence of "slow" degrees of freedom. The presence of breather localizations alters Lyapunov exponents in several ways, primarily by lowering energy of the background. This is similar in spirit to Rumpf's argument [14] for how the formation of a breather modifies the thermodynamic entropy. A less obvious but important consequence of breathers on the Lyapunov spectra was

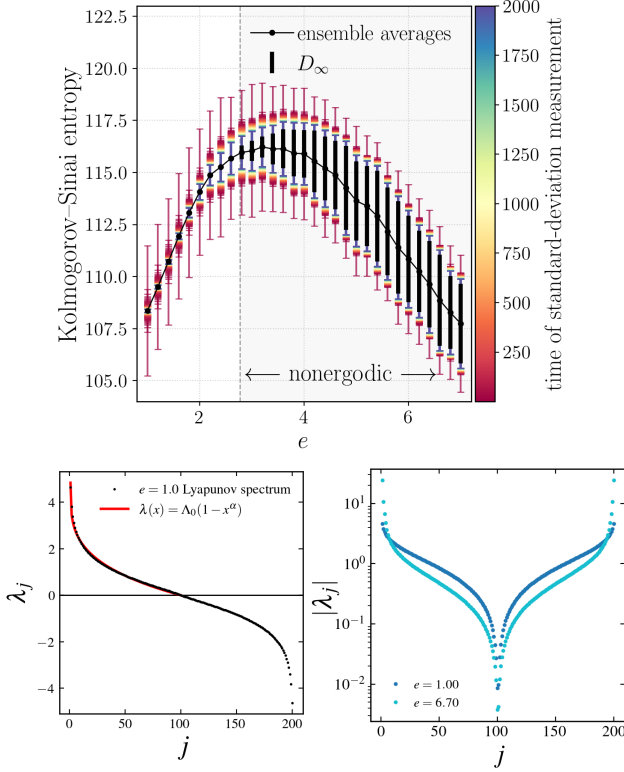


FIG. 3. **Ensemble Lyapunov spectra, Kolmogorov-Sinai entropy and standard deviation measurements.** Top: ensemble sampled Kolmogorov-Sinai entropy and standard deviation measurements across the $a = 1$ slice of the phase diagram. Vertical black bars denote predictions of D_∞ . Bottom: sample Lyapunov spectra. Left image shows the $e = 1$ spectrum and the two-parameter fit found by [15]. Right image shows the magnitudes of the same $e = 1$ spectrum contrasted with the $e = 6.7$ spectrum on a log scale.

found by Iubini and Politi [15], who showed that a region between a pair of breathers will locally have nearly conserved quantities, increasing the number of near-zero exponents.

The sensitivity of the Lyapunov spectrum to the number, size, and position of breathers makes it a well-suited observable for quantifying the dynamical heterogeneity in the DNLSE. Studying the time-dependent variance of Kolmogorov-Sinai entropy $S_{KS} = \sum_{\lambda_j > 0} \lambda_j$ across ensemble samples therefore concisely quantifies this heterogeneity from a global perspective. Kolmogorov-Sinai entropy measurements and representative Lyapunov spectra are shown in Fig. 3.

We utilize the algorithm due to Benettin *et al.* and Shimada *et al.* [16, 17] to compute the Lyapunov spectra. Details of our implementation are included in the supplementary material. For a comprehensive modern overview of the theory and methods of Lyapunov spectra, we refer to Ref. 18.

At a point $\psi(t_0)$ on the manifold \mathcal{M} , there exists a $2N - 2$ dimensional tangent space $T_{\psi(t_0)}\mathcal{M}$. The task

of a Lyapunov-spectrum measurement is to identify a decomposition of the tangent space into subspaces

$$T_{\psi(t_0)}\mathcal{M} \cong \mathcal{O}_1 \oplus \cdots \oplus \mathcal{O}_m, \quad (5)$$

where $m \leq 2N - 2$, and for any $v \in \mathcal{O}_j$ and t_0 chosen arbitrarily, we expect an infinitesimal perturbation $\bar{\psi}(t_0) = \psi(t_0) + \varepsilon v$, ($\varepsilon > 0$) to diverge from $\psi(t_0)$ at a rate

$$d(\psi(t), \bar{\psi}(t)) \approx e^{\lambda_j(t-t_0)} d(\psi(t_0), \bar{\psi}(t_0)), \quad (6)$$

where the metric between states here is

$$d(\psi(t), \bar{\psi}(t)) \equiv \frac{1}{2} \langle \psi(t) - \bar{\psi}(t) | \psi(t) - \bar{\psi}(t) \rangle \quad (7)$$

[19] and with λ_j the same for any such v . λ_j is called the characteristic Lyapunov exponent corresponding to the Oseledets subspace \mathcal{O}_j , and the dimension of \mathcal{O}_j corresponds to the multiplicity of λ_j . For initial conditions with additional symmetries (i.e., a plane-wave) the Lyapunov exponents can appear in degenerate rows corresponding to larger dimensional Oseledets spaces, however for generic initial conditions \mathcal{O}_j are typically one-dimensional.

The procedure for determining this decomposition and the corresponding Lyapunov spectrum involves an iterative process along a trajectory which frequently measures stretching factors in the immediate neighborhood of the trajectory, and yields finite-time Lyapunov exponents $\{\lambda_j(t)\}$ which together account for the chaos accumulated along the trajectory up to time t . The multiplicative ergodic theorem [20, 21] guarantees the convergence $\{\lambda_j(t)\} \rightarrow \{\lambda_j\}$ to values invariant of initial conditions when the dynamics are ergodic.

We determine the statistics of the Lyapunov spectra for a wide range of energy densities spanning the $a = 1$ slice of the phase diagram at $N = 100$. Denoting the standard deviation of the finite-time Kolmogorov-Sinai entropy at time t for states of energy e as

$$D(e, t) \equiv \text{std}_{\{\psi \in \mathcal{M}_{e, a=1}^{(N=100)}\}} [S_{KS}(\psi)]. \quad (8)$$

A sufficient condition for broken ergodicity is $\lim_{t \rightarrow \infty} D(e, t) > 0$; since if this limit were nonzero and the dynamics were ergodic it would contradict Oseledets multiplicative ergodic theorem. Furthermore, when the limit is finite its value serves as a metric of the severity of the violation of ergodicity.

We observe across all energies that the standard deviation of Kolmogorov-Sinai entropy is well described by a mixed algebraic and exponential decay law of the form

$$D(e, t) = D_\infty + K_1 \cdot t^\gamma + K_2 \exp(-t/\tau_{\text{exp}}), \quad (9)$$

where the parameters vary with energy. We fit $D(e, t)$ to this form and obtain posterior distributions for each

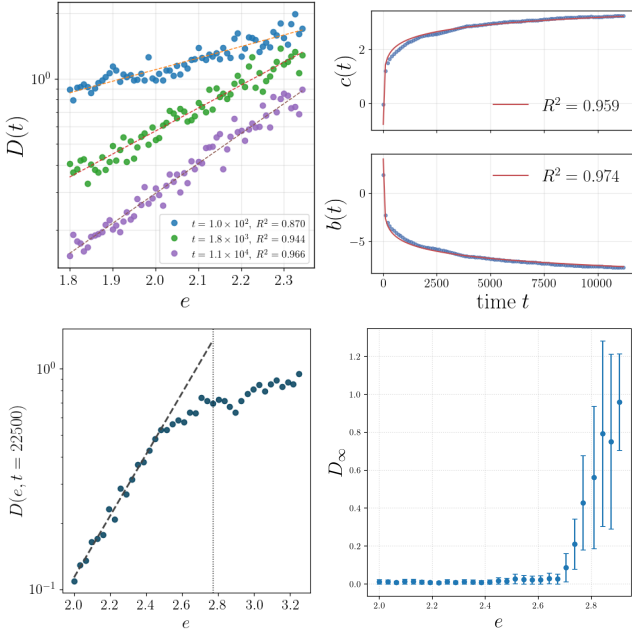


FIG. 4. **Finite-time ensemble variance and infinite time predictions of Kolmogorov-Sinai entropy vs energy density.** Top left: standard deviation of the sum of finite time positive Lyapunov exponents across 150 ensemble-sampled trajectories, after averaging over 100, 1800, and 11200 time-units respectively, with $N = 100$ and $a = 1$. The fits are exponential curves $D(t) = \exp[b + ce]$, where $b = b(t)$, $c = c(t)$ both satisfy logarithmic growth laws shown on the top right. We observe that $c(t) = c_0 + C \log(t)$, $b(t) = b_0 - B \log(t)$, with $c_0 \approx -0.32$, $b_0 \approx 2.24$, $C \approx 0.38$, $B \approx 1.07$. Bottom left: breakdown in functional form of $D(e, t)$ near $e = 2.5$. Bottom right: mean and standard deviation of posterior probability estimates of D_∞ .

parameter given the finite-time data using a Hamiltonian Monte Carlo algorithm [22]. For all $e < 2.7$, the posterior mass of D_∞ is strongly concentrated about 0, consistent with the expectation of ergodicity in this region. Near 2.7, the distributions broaden but remain within error of zero; and by $e = 2.75$ ergodicity is broken with near-certainty as the posterior density of $D_\infty = 0$ becomes negligible. Posterior means and standard deviations of D_∞ in this window are shown in Fig 4.

We find that for all $e < 2.5$, K_2 is negligible, and γ increases linearly with energy, such that

$$D(e, t) = K_1 \cdot t^{e \cdot C - B}, \quad e \lesssim 2.5. \quad (10)$$

This relation was established first from the observation of an exponential dependence in energy at fixed times, as shown in the top left of Fig. 4, giving the form $D(e) = \exp(ec + b)$. Repeating these fits across time, we find that $c = c(t)$ and $b = b(t)$ satisfy logarithmic laws of the form $c(t) = c_0 + C \log(t)$ and $b(t) = b_0 - B \log(t)$, shown in the top right of Fig. 4. Altogether, these relations reduce to Eq.(10), with $K_1 = \exp(ec_0 + b_0)$. The constants C and

B suggest a critical energy $e^* = B/C \approx 2.77$ as the value at which $\gamma \rightarrow 0$.

Importantly, e^* is outside of the window where the purely algebraic functional form is satisfied by D . In the region $e \in [2.5, 2.77]$, both K_1 and K_2 are nonzero, and the exponential term has a long characteristic timescale $\tau_{\text{exp}} \sim 7 \cdot 10^4$ time units, but does not seem to grow significantly with energy.

While the time necessary for $D \rightarrow 0$ exactly is generally infinite, one may define an effective relaxation time $\tau^{(\delta)}$ for some $\delta > 0$ as the smallest time such that $D(e, t) < \delta$ for all $t \geq \tau^{(\delta)}$. Since the term $K_2 \exp(t/\tau_{\text{exp}})$ has a long but not diverging characteristic timescale τ_{exp} , for small enough δ it is effectively negligible for the sake of determining $\tau^{(\delta)}$ and we may from Eq.(10) derive

$$\tau^{(\delta)}(e) = \exp\left(\frac{(ec_0 + b_0 - \log(\delta))/C}{e^* - e}\right) \quad (11)$$

suggesting an essential singularity in the relaxation time at e^* .

Timescales of decay in the region $e \in [2.5, 2.77]$ are extremely long, and competition between the exponential decay and algebraic decay in this region makes a precise determination of γ from the 5-parameter fit alone difficult, where distributions of the parameters are generally multimodal. It is important to clarify that Eq. (11), while confirmed in the region $e < 2.5$, is an extrapolation assuming that the algebraic term holds that exact form in the critical window $e \in [2.5, 2.77]$; however, to prove this will require further investigation.

Even if γ cannot be cleanly resolved as of yet for $e \in [2.5, 2.77]$, the fact that D_∞ is predicted to become nonzero at an energy within error of e^* gives us confidence that the extrapolated linear vanishing of γ is correct, and that the divergence in relaxation times at e^* is driven by the extrapolated behavior of the algebraic decay.

In conclusion, through a study of the convergence rates of Kolmogorov-Sinai entropy across a large set of micro-canonical ensemble samples, our results significantly contribute to an understanding of the properties of the ergodicity transition in the DNLSE. In the sense that the transition from ergodic to nonergodic dynamics can be considered a phase transition, the asymptotic variance of Kolmogorov-Sinai entropy $\lim_{t \rightarrow \infty} D(e, t) = D_\infty(e)$ may be considered a dynamical order parameter; where $D_\infty = 0$ in the ergodic phase and $D_\infty > 0$ in the non-ergodic phase. Additionally, it seems likely that D_∞ emerges continuously from zero, so that in this sense the dynamical transition is continuous.

While demonstrated for the DNLSE, the provided framework should apply quite generally to systems that support both ergodic and nonergodic behavior. Beyond the binary classification of a state as ergodic or not, this method could be useful in establishing universality

classes of nonergodic systems, classified by the form of divergence in relaxation times.

PFC and WAB thank the support of startup funds from Emory University.

* benalcazar@emory.edu

- [1] Giacomo Gradenigo, Stefano Iubini, Roberto Livi, and Satya N. Majumdar, Condensation transition and ensemble inequivalence in the discrete nonlinear schrödinger equation, *The European Physical Journal E* **44**, 10.1140/epje/s10189-021-00046-5 (2021).
- [2] K. Ø. Rasmussen, T. Cretegny, P. G. Kevrekidis, and Niels Grønbech-Jensen, Statistical mechanics of a discrete nonlinear system, *Phys. Rev. Lett.* **84**, 3740–3743 (2000).
- [3] Thudiyangal Mithun, Yagmur Kati, Carlo Danieli, and Sergej Flach, Weakly nonergodic dynamics in the gross-pitaevskii lattice, *Phys. Rev. Lett.* **120**, 184101 (2018).
- [4] D. N. Christodoulides and R. I. Joseph, Discrete self-focusing in nonlinear arrays of coupled waveguides, *Optics Letters* **13**, 794–796 (1988).
- [5] Qidong Fu, Peng Wang, Yaroslav V. Kartashov, Vladimir V. Konotop, and Fangwei Ye, Nonlinear threshold pumping: Solitons and transport breakdown, *Physical Review Letters* **128**, 10.1103/physrevlett.128.154101 (2022).
- [6] Alexander V. Milovanov, Jens Juul Rasmussen, and Guilhem Dif-Pradalier, Self-consistent model of the plasma staircase and nonlinear schrödinger equation with sub-quadratic power nonlinearity, *Phys. Rev. E* **103**, 052218 (2021).
- [7] Dahirou Mahmoud, Saïdou Abdoukary, L.Q. English, and Alidou Mohamadou, Propagation of acoustic solitons in a nonlinear left-handed transmission line, *Wave Motion* **139**, 103597 (2025).
- [8] Nora Molkenhuth, Shuangwei Hu, and Antti J. Niemi, Discrete nonlinear schrödinger equation and polygonal solitons with applications to collapsed proteins, *Phys. Rev. Lett.* **106**, 078102 (2011).
- [9] Herbert Federer, *Geometric Measure Theory*, 1st ed., Classics in Mathematics (Springer Berlin, Heidelberg, Berlin; Heidelberg, 1996) pp. iv+677, originally published as volume 153 of *Grundlehren der mathematischen Wissenschaften*.
- [10] Roberto Franzosi, Geometric microcanonical thermodynamics for systems with first integrals, *Phys. Rev. E* **85**, 050101 (2012).
- [11] Arthur Sard, The measure of the critical values of differentiable maps, *Bull. Amer. Math. Soc.* **48**, 883–890 (1942).
- [12] Nicholas Metropolis, Arianna W. Rosenbluth, Marshall N. Rosenbluth, Augusta H. Teller, and Edward Teller, Equation of state calculations by fast computing machines, *The Journal of Chemical Physics* **21**, 1087–1092 (1953).
- [13] W. K. Hastings, Monte Carlo sampling methods using Markov chains and their applications, *Biometrika* **57**, 97–109 (1970).
- [14] Benno Rumpf, Simple statistical explanation for the localization of energy in nonlinear lattices with two conserved quantities, *Phys. Rev. E* **69**, 016618 (2004).
- [15] Stefano Iubini and Antonio Politi, Chaos and localization in the discrete nonlinear schrödinger equation, *Chaos, Solitons & Fractals* **147**, 110954 (2021).
- [16] Giancarlo Benettin, Luigi Galgani, Antonio Giorgilli, and Jean-Marie Strelcyn, Lyapunov characteristic exponents for smooth dynamical systems and for hamiltonian systems; a method for computing all of them. part 1: Theory, *Meccanica* **15**, 9–20 (1980).
- [17] Ippei Shimada and Tomomasa Nagashima, A numerical approach to ergodic problem of dissipative dynamical systems, *Progress of Theoretical Physics* **61**, 1605–1616 (1979), <https://academic.oup.com/ptp/article-pdf/61/6/1605/5183075/61-6-1605.pdf>.
- [18] Francesco Ginelli, Hugues Chaté, Roberto Livi, and Antonio Politi, Covariant lyapunov vectors, *Journal of Physics A: Mathematical and Theoretical* **46**, 254005 (2013).
- [19] Iva Březinová, Lee A. Collins, Katharina Ludwig, Barry I. Schneider, and Joachim Burgdörfer, Wave chaos in the nonequilibrium dynamics of the gross-pitaevskii equation, *Phys. Rev. A* **83**, 043611 (2011).
- [20] V.I. Oseledets, A multiplicative ergodic theorem. characteristic lyapunov exponents of dynamical systems, *Trans. Moscow Math. Soc.* **19**, 179–210 (1968).
- [21] SIMION FILIP, Notes on the multiplicative ergodic theorem, *Ergodic Theory and Dynamical Systems* **39**, 1153–1189 (2017).
- [22] Michael Betancourt, A conceptual introduction to hamiltonian monte carlo (2018), arXiv:1701.02434 [stat.ME].